Hydrogen peroxide and oxygen reduction studies on Pt stepped surfaces: Surface charge effects and mechanistic consequences

Valentín Briega-Martos, Enrique Herrero, Juan M. Feliu

PII: S0013-4686(19)32324-2

DOI: https://doi.org/10.1016/j.electacta.2019.135452

Reference: EA 135452

To appear in: *Electrochimica Acta*

Received Date: 23 September 2019

Revised Date: 30 November 2019

Accepted Date: 4 December 2019

Please cite this article as: Valentí. Briega-Martos, E. Herrero, J.M. Feliu, Hydrogen peroxide and oxygen reduction studies on Pt stepped surfaces: Surface charge effects and mechanistic consequences, *Electrochimica Acta* (2020), doi: https://doi.org/10.1016/j.electacta.2019.135452.

Hydrogen peroxide and oxygen reduction studies on Pt stepped surfaces: surface charge effects and mechanistic consequences

Valentín Briega-Martos[1], *Enrique Herrero*[1*], *Juan. M. Feliu*[1]

[1]Instituto de Electroquímica, Universidad de Alicante, Apdo. 99, E-03080 Alicante, Spain

*Corresponding author: herrero@ua.es

Abstract

The hydrogen peroxide reduction reaction (HPRR) is investigated on Pt(111) as well as on Pt(S)[(n-1)(111) × (110)] and Pt(S)[n(111) × (100)] stepped surfaces in 0.1 M $HClO_4$ by means of voltammetric studies using the hanging meniscus rotating disk electrode (HMRDE) configuration. Results point out that there is a direct correlation between the potential value ($E_{inhibition}$) at which the inhibition of the HPRR at low potential starts and the local potential of maximum entropy (pme) for the terraces. In addition, there is also a correspondence between the potential of the peak (E_{peak}) that appears at E < 0.3 V vs. RHE for stepped surfaces and the local pme for the steps. Additional experiments for stepped surfaces from acidic to neutral pH confirm this correlation since $E_{inhibition}$ shifts 0.059 V per pH units towards more positive potentials, which is the same observed behavior for the pme from laser-induced temperature-jump experiments. However, adsorbed OH can influence this trend when the pme values are near the region of adsorption of these species. The effect of surface charge on the structure of interfacial water can also influence the current inhibition as inferred from measurements in alkaline media. Finally, ORR measurements and the differences observed with the HPRR results in the same conditions suggest that the formation of

H_2O_2 intermediate is less favored as the pH is increased, and therefore a previous bifurcation point in the mechanism should exist.

Keywords: platinum electrodes; oxygen reduction reaction; hydrogen peroxide reduction reaction; single crystal surfaces, effect of the surface charge.

1. Introduction

The oxygen reduction reaction (ORR) is one of the most important reactions in the electrocatalysis field since it takes part in several technologies such as fuel cells and metal-air batteries. It involves a four-electron transfer process in which oxygen is converted to water (equation 1):

$$O_2 + 4H^+ + 4e^- \rightarrow 2H_2O \quad E^0 = 1.229\ \text{V vs. SHE} \tag{1}$$

Oxygen may also undergo a two-electron reduction process to form hydrogen peroxide, and depending on the experimental conditions, hydrogen peroxide can either be the final product, or go through another two-electron reduction process to form water as the final product. Both reaction pathways can also occur simultaneously [1].

One of the main drawbacks of fuel cell technology is the sluggish kinetics of the ORR. Pt nanoparticles supported on carbon black (Pt/C) have been the commonly used electrocatalyst for both ORR and hydrogen oxidation reaction (HOR) at the cathode and the anode, respectively, since Pt is the best pure metal for these reactions [2-4]. However, even for Pt, there is a considerable overpotential associated with the ORR. Therefore, it is necessary to perform fundamental studies in order to understand the ORR mechanism and the ways to improve its activity by the development of new electrocatalysts and changing the conditions of the different fuel cell set-ups.

During the last 20 years, a high number of theoretical works have been published in which different ORR mechanisms are proposed [5-14]. However, it has not been possible to certainly establish the identity of the intermediate species in the different conditions.[1, 15] The main reasons are that the physical and/or chemical properties of the ORR intermediates cannot be measured using the usual experimental techniques and that the equipment sensitivity is not high enough to detect them. This is

mainly because of the short lifetime and low coverage of most of the intermediates [16]. This makes necessary to devise different experimental strategies to what has been performed to date, in order to obtain new information about the mechanism of this reaction.

In recent works by Gomez-Marín *et al*., new strategies using cyclic voltammetry studies were carried out in order to obtain new insights about the ORR mechanism [1, 17]. These investigations comprise measurements with different initial potentials and holding times and other different experimental conditions, such as O_2-diluted solutions, slow and fast rotation rates, quiescent solutions and measurements within a potential region up to 1.15 V vs. RHE. All these experiments were carried out on Pt(111), and from the observed results, the authors proposed the existence of a soluble intermediate, namely $OOH^{\bullet}$ species. Further experiments under non-steady-state conditions for polycrystalline Pt with different resting times at high potentials and with different scan rates were also performed [18]. From these results, the authors suggested that the $OOH^{\bullet}$ soluble species are formed in an initial and fast chemical reaction, and equilibrium is reached in such a way that no currents are measured at potentials more positive than the onset potential. Once the onset potential is attained, this intermediate species should be reduced yielding the next reaction intermediates.

In our group, different approaches were used for obtaining more information about the ORR mechanism. ORR measurements on Pt basal planes and Pt stepped surfaces were carried out in $NaF/HClO_4$ mixtures, which allow the preparation of buffer solutions in the pH range from 1 to ca. 6 in the absence of anion specific adsorption [19, 20]. On the one hand, in light of the different behavior observed for Pt(111) and the other two basal planes and also for stepped surfaces, it was proposed that there is an effect of the surface charge and the interfacial water structure on the ORR

electrocatalysis [19]. On the other hand, a gradual diminution of the limiting current density is observed as solution pH is increased from 3 to ca. 5.5. After discarding diffusion control by H_3O^+ and the formation of H_2O_2 as the final product, it was proposed that this diminution is due to a bifurcation point in the mechanism before the formation of hydrogen peroxide. This bifurcation point would be the formation of the $OOH^\bullet$ species previously proposed by Gómez-Marín et al.[19]

Further experiments investigating the hydrogen peroxide reduction reaction (HPRR) in Pt(111) at different pH values were performed [21]. The study of the HPRR is of paramount importance since H_2O_2 is one of the possible ORR intermediates. Results also pointed out a surface charge effect on this reaction, since the inhibition at low potentials starts at the same potential for all the pH values. This potential is close to the potential of maximum entropy (pme) of Pt(111), which is, in turn, intimately related to the potential of zero free charge (pzfc) [22]. In addition, there is no diminution of the limiting current density inhibition in the plateau region for the HPRR, in contrast to the ORR, and this supports the idea that a different intermediate, other than H_2O_2, is formed in these conditions. The ORR and the HPRR were also investigated in the presence of bromide anions, and while the limiting current density for the HPRR was strongly inhibited by bromide adsorption for all the studied pH values, there was no inhibition for the ORR at pH > 2 in comparison with the case without bromide [20]. The behavior of ORR and HPRR with varying the ionic strength of the solution is also different. All these results suggest that the ORR can proceed through different routes depending on the conditions, and $OOH^\bullet$ as the bifurcation point would be a critical point that controls which pathway will take place [20].

In order to unambiguously identify the ORR intermediates, shell-isolated nanoparticle-enhanced Raman spectroscopy (SHINERS) measurements were carried out

for this reaction on the three Pt basal planes in acid and alkaline media [23]. By using this technique the $OOH^{\bullet}$ intermediate could be identified on Pt(111) surface in acid media. In alkaline media, O_2^- was identified for the three basal planes. Multi-bounce attenuated total reflection infrared (ATR-IR) spectroelectrochemical measurements during the ORR on Pt nanoparticle catalyst in acidic media also allowed identifying $OOH^{\bullet}$ species during the ORR mechanism [24]. The confirmation of the presence of this intermediate supports the idea that it can constitute a bifurcation point mechanism.

In this work, additional hanging meniscus rotating ring disk electrode (HMRDE) studies with Pt stepped surfaces at different pH values and different working solution compositions for HPRR are performed to gain insight into the reaction mechanism. Measurements for the ORR also presented, in order to obtain more information about the effect of the surface charge properties on the electrocatalysis of these reactions and to find new pieces of evidence, which supports the hypothesis suggested in the previous works by the comparison of the results for both reactions.

2. Experimental

Experiments were performed in a two-compartment electrochemical glass cell with three electrodes following the general procedure described in [25]. The Pt single crystals used as working electrodes were prepared from small Pt beads of ca. 2 mm in diameter, in accordance with the method described by Clavilier et al. [26]. In this work, the three Pt basal planes as well as different Pt(S)[(n-1)(111) × (110)] and Pt(S)[n(111) × (100)] stepped surfaces were employed. Prior to the electrochemical measurements, the working electrode was flame annealed in a propane-flame, cooled in Ar/H_2 (3:1) reducing atmosphere and protected with an ultrapure water drop saturated with these gases for its transference to the electrochemical cell. It has been reported that

by using this cooling atmosphere the experimental surface structures are in agreement with the nominal topographies [27]. The counter electrode was a platinum coiled wire cleaned by flame annealing and quenched with ultrapure water. The reference electrode used for solutions without NaF was a reversible hydrogen electrode (RHE), while in the case of solutions containing NaF the reference electrode was a Ag/AgCl, KCl (saturated) electrode. More details about the use of this electrode are given in ref. [19]. Potential values have been transformed to RHE, or SHE, when required.

Working solutions were prepared using concentrated $HClO_4$ (Merck, for analysis), NaF (Merck, Suprapur, 99.99%), $NaOH \cdot H_2O$ (Merck, Suprapur, 99.99%), $KClO_4$ (Merck, for analysis) and ≥ 30% H_2O_2 solution (Fluka, TraceSELECT® Ultra, for trace analysis). Ar, H_2, and O_2 (N50, Air Liquide) gases were employed. Ultrapure water (Elga PureLab Ultra, 18.2 MΩ cm) was used for glassware cleaning and the preparation of the solutions. The compositions of the supporting electrolytes used for the different working solutions are specified in table S1.

A signal generator EG&G PARC and eDAQ EA161 potentiostat with and eDAQ e-corder ED401 recording system were used for the electrochemical measurements. Experiments in hydrodynamic conditions were carried out in the HMRDE configuration using an EDI101 rotating electrode. The rotating rate was controlled by a Radiometer CTV 101. All experiments were performed at room temperature.

3. Results and discussion

Hydrogen peroxide reduction reaction (HPRR) in 0.1 M $HClO_4$

Figure 1A shows the voltammetric profiles for different Pt(S)[(n-1)(111) × (110)] surfaces in 0.1 M $HClO_4$ in presence of H_2O_2 under hydrodynamic conditions. The HPRR and the hydrogen peroxide oxidation reaction (HPOR) take place under diffusion control at potentials below 0.8 V and above 1.0 V vs. RHE, respectively. The charge transfer controlled regions for both reactions overlap and take place between these potential values [28]. An inhibition of HPRR can be observed at low potentials: the potential value ($E_{inhibition}$) at which current densities start decreasing below the limiting current density (j_{lim}) moves to more positive potentials as the length of the (111) terraces is shortened (i.e., the step density increases). The value of $E_{inhibition}$ is illustrated in figure 1B, and it is identified as the potential value in which the calculated first derivative of the current density starts being different from zero. For Pt(111), it was observed that $E_{inhibition}$ is directly related to the interfacial charge and corresponds approximately with the pzfc of the interface [21]. Thus, it appears that the surface charge is an important variable in determining the reactivity. It should be reminded that for metals with adsorptive properties, such as platinum, two potentials of zero charge can be established [29]. The pzfc is the potential at which the surface charge is zero and is equivalent to the potential of zero charge (pzc) for metals without specific adsorption properties, such as gold. For platinum, the pzfc is not measurable, due to the interference of the adsorption reactions (i.e., hydrogen and anions). The other potential, the potential of zero total charge (pztc), which is measurable, is the potential at which the surface charge plus the charge exchanged in the adsorption processes is zero. In general, the pztc of platinum lies in the region where the charge exchanged in the process of adsorption of hydrogen is equal to that

corresponding to the adsorption of anions, that is, in the region where both coverages are equal (and generally small). Another related potential is the pme, which is the potential value in which the water adlayer is totally disordered. As the orientation of water molecules depends on the interaction of water dipoles with the electric field at the interface, the pme is expected to be close to the pzfc.

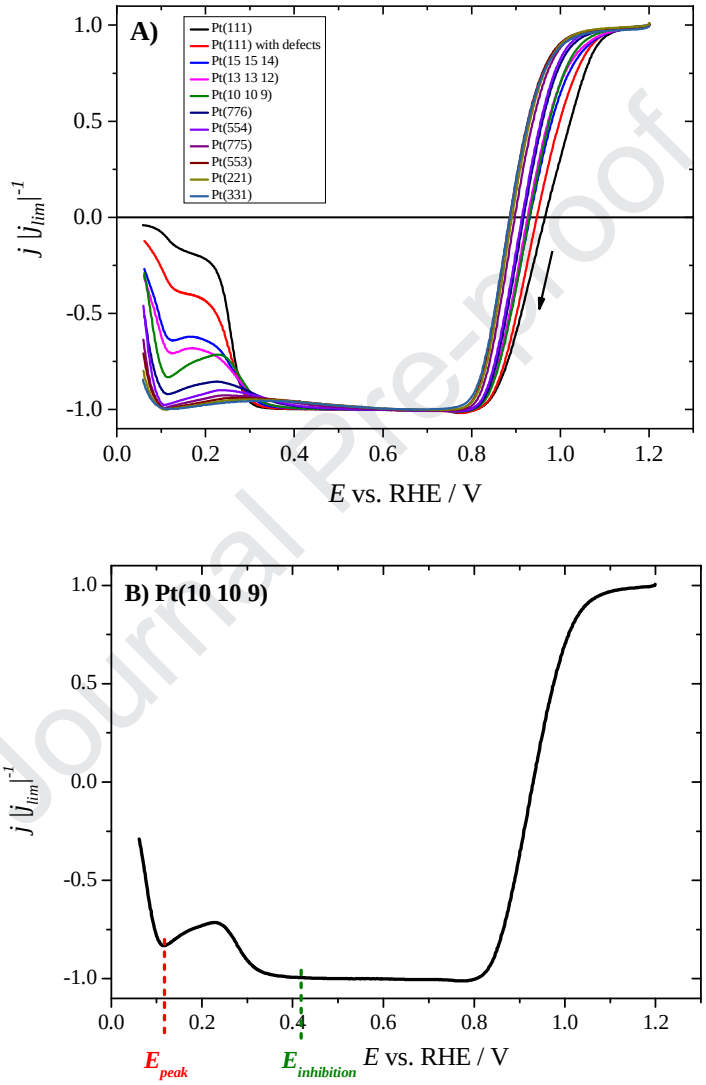

Figure 1: Normalized polarization curves for the HPRR and HPOR on different Pt(S)[(n-1)(111) × (110)] stepped surfaces in Ar-saturated 0.1 M $HClO_4$ and 1.7 mM H_2O_2 (A). Normalized polarization curve for Pt(10 10 9) illustrating the position of $E_{inhibition}$ and E_{peak} values (B). Scan rate: 50 mV s^{-1}, rotation rate: 2500 rpm. Original data prior to normalization are shown in Figure S1.

García-Araez et al. investigated the potential-dependent water orientation on stepped surfaces with (111) terraces by using laser-induced temperature-jump

experiments to determine the pme [30]. These experiments pointed out the existence of local pme values for both terrace and step sites. Analogous conclusions were drawn in a previous investigation of the pzc on stepped surfaces by using N_2O reduction: the maximum in the N_2O reduction current can be correlated with the pztc since N_2O is a neutral molecule and its adsorption to the metal surface is weak [31]. Thus, at high coverage of hydrogen or anions, the reduction of N_2O is inhibited. The presence of two peaks at different potential regions during N_2O reduction suggested the existence of local pztc values for terraces and step sites. While the trends for the local pztc and pme of step sites agree for both methods, there is a discrepancy in the case of terrace sites: pme values determined by laser-induced temperature-jump experiments increase as the step density is increased [30], while the opposite behavior is observed for pztc values obtained by N_2O reduction [31]. As can be seen in figure 2, the trend observed in this work for the hydrogen peroxide reduction is in good agreement with the obtained results for pme values. As the step density increases, $E_{inhibition}$ values shift to higher potentials. Estimation of pztc of terraces using N_2O reduction is more complicated since the peak in the reduction currents is very broad and for short terraces, the contribution from terraces is very small when compared with the contribution from step sites making difficult the determination of the peak potential for terraces. Therefore, the present results suggest that the determination of local pzc in terraces sites by laser-induced temperature-jump experiments is a more reliable method than N_2O reduction and that hydrogen peroxide reduction allows a direct an easy estimation of the local pzfc of terraces on platinum surfaces. This is because, on the contrary to N_2O reduction, HPRR becomes diffusion controlled at very positive potentials and as a result the limiting current density is always achieved for all the orientations. The explanation given in [30] for the pme variation as a function of step density is that steps disrupt the formation of

extended water networks making easier the inversion of water dipoles to the orientation with hydrogen directed to the metal surface. The higher the step density is, the higher this effect is. The inhibition observed in the HPRR can be related then to changes in the orientation of the interfacial water molecules: at potential values more negative than the local pme for terraces the water molecules are oriented with the hydrogen atoms pointing toward the surface, and this configuration inhibits the HPRR.

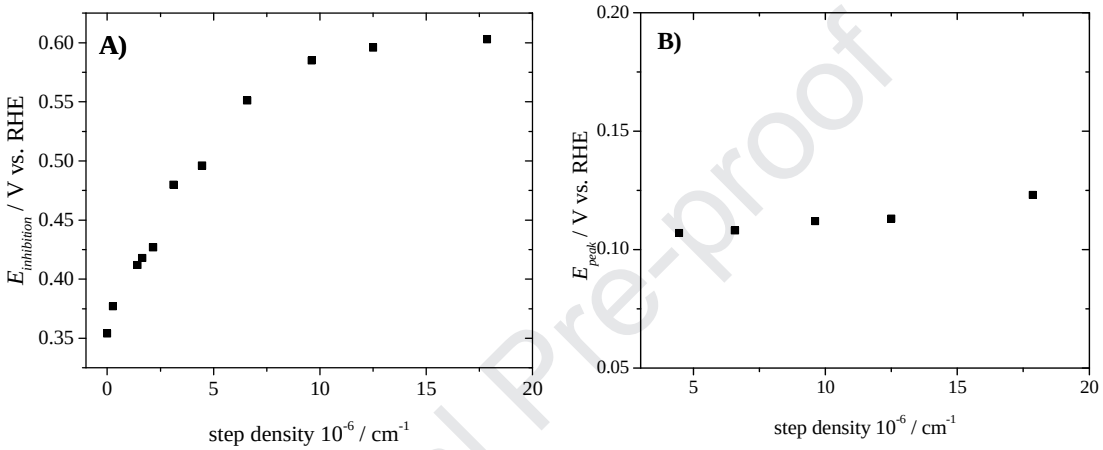

Figure 2: $E_{inhibition}$ (A) and E_{peak} (B) associated with step density for Pt(S)[(n-1)(111) × (110)] stepped surfaces in Ar-saturated 0.1 M $HClO_4$ and 1.7 mM H_2O_2.

Another remarkable feature in figure 1 is the appearance of a reduction peak at potential values (E_{peak}) between 0.1 and 0.2 V vs. RHE (see figure 1). The peak intensity increases with step density, indicating that the origin of this signal is related to the reactivation of the HPRR due to the presence of steps [21]. The small contribution observed in Pt(111) is due to the presence of defects on the surface. This signal increases when a defective Pt(111) electrode is used, which reinforces the assignment of this signal to the defects. It should be mentioned that, although the number of defects in the high-quality Pt(111) electrode used in this work is well below the 1%, the catalytic activity related to these sites could be significantly high. Thus, the effect due to the presence of defects on the surface in the curves is higher than that expected from the actual ratio of defects. This peak appears in the same potential region for the

voltammetric peak traditionally attributed to hydrogen adsorption on step sites, as can be seen in the cyclic voltammetric profiles in absence of hydrogen peroxide (figure 3). Measurements at several scan rates for different stepped surfaces were performed, and also for the positive-going scan (see figure S8 in the Supplementary Materials). $E_{inhibition}$ and E_{peak} are independent of both scan rate and direction, and therefore the correspondences established in this work are valid. The reactivation of the HPRR at E_{peak} by the step sites can be also explained in terms of the interfacial water structure. García-Aráez et al. observed that the local pme for step sites also lies in the same potential region as the voltammetric peak for steps [30]. It should be stressed that there is not a local inversion of water molecules adsorbed on steps, with water on terraces remaining with the hydrogen towards the metal [30] and different from the orientation of water on the steps. Instead, there is a strong cooperative phenomenon: the local reorientation of water molecules on steps sites triggers the reorientation of a significant fraction of the water adlayer on the whole surface. Therefore, although at potentials more negative than the local pme for the terraces (but more positive than the local pme for steps) the water molecules are oriented with the hydrogen pointing toward the surface and thus inhibiting the HPRR, as the potential diminishes and approaches that of the local pme for steps, the water molecules of practically the whole surface (as mentioned above) reorientate with the oxygen pointing toward the surface, and the HPRR is reactivated again. At potentials more negative than the local pme for steps the water molecules orientate again with the hydrogen pointing toward the surface and the HPRR is inhibited. The changes in the interfacial water structure are evidenced by laser-induced temperature-jump experiments [30].

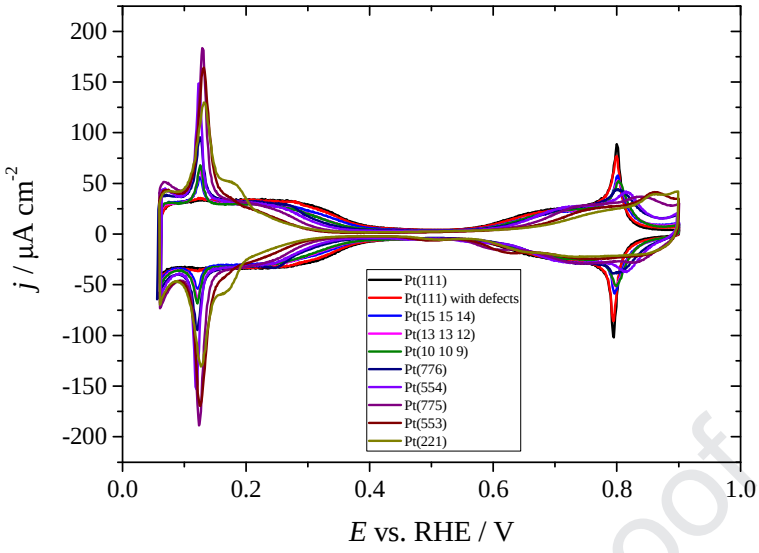

Figure 3: Voltammetric profiles for Pt(S)[(n-1)(111) × (110)] stepped surfaces in Ar-saturated 0.1 M $HClO_4$ solution. Scan rate: 50 mV s^{-1}.

Very similar behavior is observed for N_2O reduction, and in this case the signal was attributed to N_2O reduction at step sites and the peak potential value corresponds to the local pztc [31]. The determination of local pzc for step sites for long terraces is more difficult in the case of hydrogen peroxide reduction since the peak is superimposed with the inhibition associated to the terraces, and therefore E_{peak} appears at more positive potentials than the local pzc for steps. However, for shorter terraces, it can be seen that, although the inhibition starts at more positive potentials, current densities decrease to a lower extent, probably because in this cases the changes in water structure are not as sudden as for surfaces with longer terraces, since it can be seen in the laser-induced temperature-jump experiments that the transients change more gradually in the case of shorter terraces. Consequently, the correspondence between the E_{peak} and the local pzc for steps is more reliable for shorter terraces because the superimposed current inhibition is much lower, or in other words, in these cases the steps are able to change the orientation of interfacial water molecules more effectively. Local pme step values determination by laser-induced temperature-jump experiments and local pztc step

investigation by N_2O reduction pointed out that these values are approximately constant for long terraces, but for the shorter terraces ($n < 5$) they increase slightly with step density [30, 31]. The same trend can be observed in this work for hydrogen peroxide reduction: for $n < 5$ the potential value for the peak potential becomes gradually more positive as the terrace is shortened. Figure 2 summarizes the local properties estimated by using the hydrogen peroxide reduction.

Similar studies were carried out for Pt(S)[n(111) × (100)] stepped surfaces (Figure 4A). The selected upper potential was 0.9 V vs. RHE because these surfaces get disordered at higher potentials due to the oxidation process of the surface and the voltammetric peak for (110) defects becomes more pronounced. The same trend for $E_{inhibition}$ can be observed: the shorter the terrace is, the higher the value for $E_{inhibition}$ is measured. However, in this case, the peak observed at low potentials appears at a potential value around 0.28 V vs. RHE. This value agrees with the potential for the step voltammetric peak for these orientations, as can be seen in the cyclic voltammetry in the absence of H_2O_2 in Figure 4B, and also with the local pme for steps as determined in [30]. Finally, it is important to mention that the peak that can be observed around 0.12 V vs. RHE may arise from (110) defects present on this surface, or, in surfaces with very short terraces, due to changes in the electronic properties because of the proximity between the steps. As can be seen in figure 4B, the hydrogen adsorption/desorption regions in the cyclic voltammetric profiles in the absence of H_2O_2 for the surfaces with higher step density change appreciably.

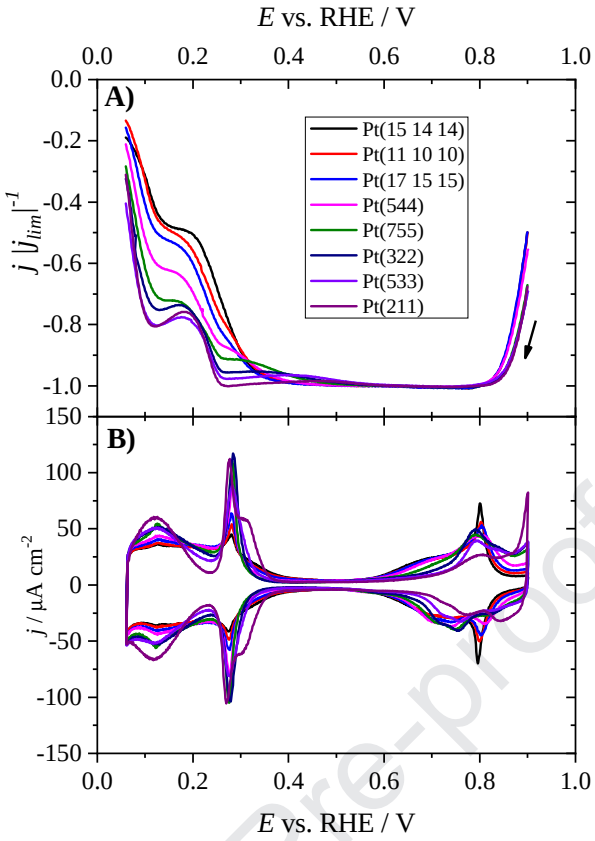

Figure 4: Normalized polarization curves for the HPRR on different Pt(S)[n(111) × (100)] stepped surfaces in Ar-saturated 0.1 M $HClO_4$ and 1.7 mM H_2O_2; scan rate: 50 mV s^{-1}, rotation rate: 2500 rpm (A) and voltammetric profiles for the same surfaces in Ar-saturated 0.1 M $HClO_4$; scan rate: 50 mV s^{-1} (B). Original data prior to normalization are shown in Figure S2.

The results from this section point out, for the first time, that there is a direct relationship between $E_{inhibition}$ for the HPRR and the local pme for terraces on Pt stepped surfaces with terraces with (111) orientation and steps with (110) or (100) symmetry. Furthermore, it can be observed that there is also a correspondence between E_{peak} and the local pme for steps.

Hydrogen peroxide reduction reaction (HPRR) at different pH values

Hydrogen peroxide reduction on Pt(S)[(n-1)(111) × (110)] at different pH values was also studied and results are presented in Figure 5. Regarding the terrace sites, the observed behavior for long terraces is the same as that recorded for Pt(111) [21]: $E_{inhibition}$ moves 0.059 × pH V to more positive values in the RHE scale. Specifically, the

$E_{inhibition}$ is pH-independent in the SHE scale and is very close to the local pme of terraces. This pH dependence was already observed also for the pme by laser-induced temperature-jump experiments on Pt(111) at different pH solutions [22]. A recent study also pointed out that the peak for N_2O reduction and the potential for complete current inhibition for peroxodisulfate anion reduction on Pt(111) are pH-independent in the SHE scale and both lie near the pzfc [32].

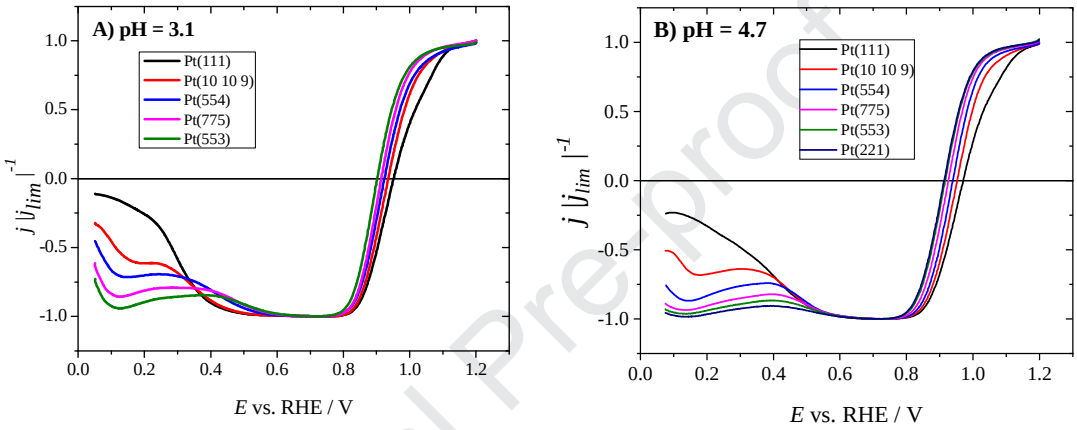

Figure 5: Normalized polarization curves for the HPRR and HPOR on different Pt(S)[(n-1)(111) × (110)] stepped surfaces in 1.7 mM H_2O_2 Ar-saturated solutions with pH = 3.1 (A) and pH = 4.7 (B) prepared with NaF/$HClO_4$ mixtures; scan rate: 50 mV s^{-1}, rotation rate: 2500 rpm. Original data prior to normalization are shown in Figure S3.

For short terraces the dependence of $E_{inhibition}$ with pH is different. For n < 7, $E_{inhibition}$ is the same in the RHE scale for all the pH values. Determination of pme in alkaline solutions suggested that there is a buffering effect by OH adsorption on the measured pme values and thus they do not follow the same trend as in acid media [22]. OH adsorption can also influence the local pme of terraces on stepped surfaces as well as $E_{inhibition}$ for the HPRR, since the pme is shifted to more positive potentials in the RHE scale in comparison with Pt(111) as the step density is increased. It can be seen in figure 2 that $E_{inhibition}$ reaches an almost constant value (ca.0.6 V vs. RHE) as it gets closer to the potential region for OH adsorption. Therefore, for stepped surfaces with short terraces, $E_{inhibition}$ will be the same in the RHE scale for all pH values due to the

influence of OH adsorption, since the latter takes place at the same potential in the RHE scale for all pH values. A similar effect was observed when comparing $E_{inhibition}$ for the HPRR at pH = 5.5 and pH = 13 on Pt(111): despite the important pH difference, $E_{inhibition}$ is the same in the RHE scale in both cases because of the buffering effect of adsorbed OH [21]. In addition, when the HPRR on Pt(100) and Pt(110) is investigated at different pH values, there are no changes in terms of $E_{inhibition}$ (figure 6). This is because adsorbed OH on Pt(111) is relatively labile and its coverage below ca. 0.7 V vs. RHE is almost negligible. On the other hand, for both Pt(100) and Pt(110) the desorption takes place at more negative potentials and probably is less affected by the electrode potential and water structure. As a result, adsorbed OH can affect the pme on these surfaces on the whole pH range giving rise to a constant behavior. For stepped surfaces with intermediate terrace lengths, an intermediate behavior is observed: at low pH values an increase of $E_{inhibition}$ in the RHE scale is observed, but it remains constant in the RHE scale at pH values where OH adsorption can affect the pme value. As a result, it can be seen in Figure 5 that $E_{inhibition}$ is practically the same in the RHE scale for all the studied stepped surfaces at pH = 4.7.

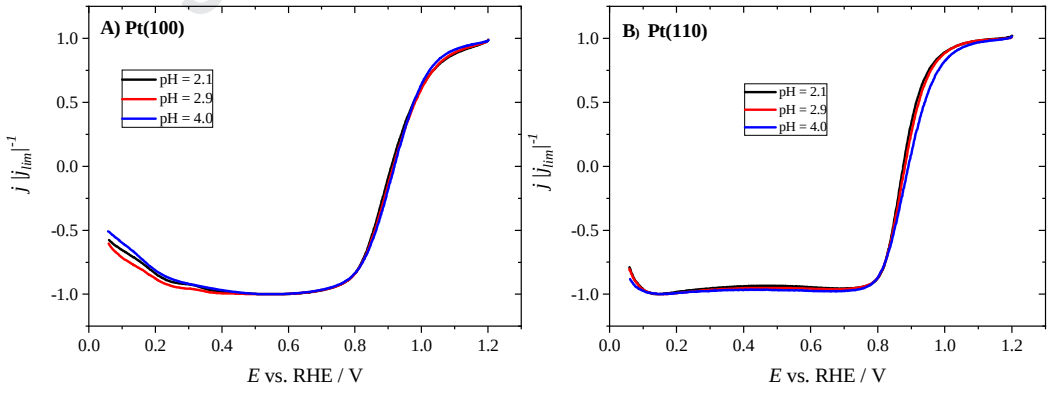

Figure 6: Normalized polarization curves for the HPRR and HPOR on different Pt(S)[(n-1)(111) × (110)] stepped surfaces in 1.7 mM H_2O_2 Ar-saturated solutions with pH < 5.5 prepared with NaF/$HClO_4$ mixtures on Pt(100) (A) and Pt(110) (B); scan rate: 50 mV s^{-1}, rotation rate: 2500 rpm. Original data prior to normalization are shown in Figure S4.

Figure 7 shows a comparison between the results in RHE and SHE scale for different stepped surfaces for illustrating the three different behaviors mentioned above: a surface with long terraces and no variation of $E_{inhibition}$ with pH in the SHE scale, a second one with short terraces and no variation of $E_{inhibition}$ with pH in the RHE scale and finally a third one with an intermediate situation. It can be seen that for Pt(10 10 9) the variation in the RHE scale of $E_{inhibition}$ with pH is 0.059 V per pH unit (they have the same value in the SHE scale), while for Pt(553) $E_{inhibition}$ is constant in the RHE scale since the presence of OH is determining its potential value. The higher reduction currents for pH = 1 are probably due to the effects of a different water structure. In the case of Pt(554) surface, there is a shift of $E_{inhibtion}$ of 0.059 V per pH unit in the RHE scale from pH 1.0 to pH 3.1 (same value in the SHE scale), but the shift is lower from pH = 3.1 to pH = 4.7 due to OH adsorption starts to play a role in the latter pH. The precise determination of pme values by laser-induced temperature-jump method in the case of stepped surfaces at more neutral values is more complicated since results are slightly affected by slow relaxation phenomena [30]. Therefore, a direct comparison between $E_{inhibtion}$ and pme is more difficult in this case. It can be observed that the determination of the pme is especially complicated in the case of very short terraces, and for Pt(221) it even seems that no transient takes place at high potentials [30]. This could be due to the presence of a high number of steps that disrupt the water network, but it can also be related to the fact that in this case the pme would lie in the region of OH adsorption and therefore the pme could be affected by the latter, and this would be in agreement with the present results for $E_{inhibition.}$

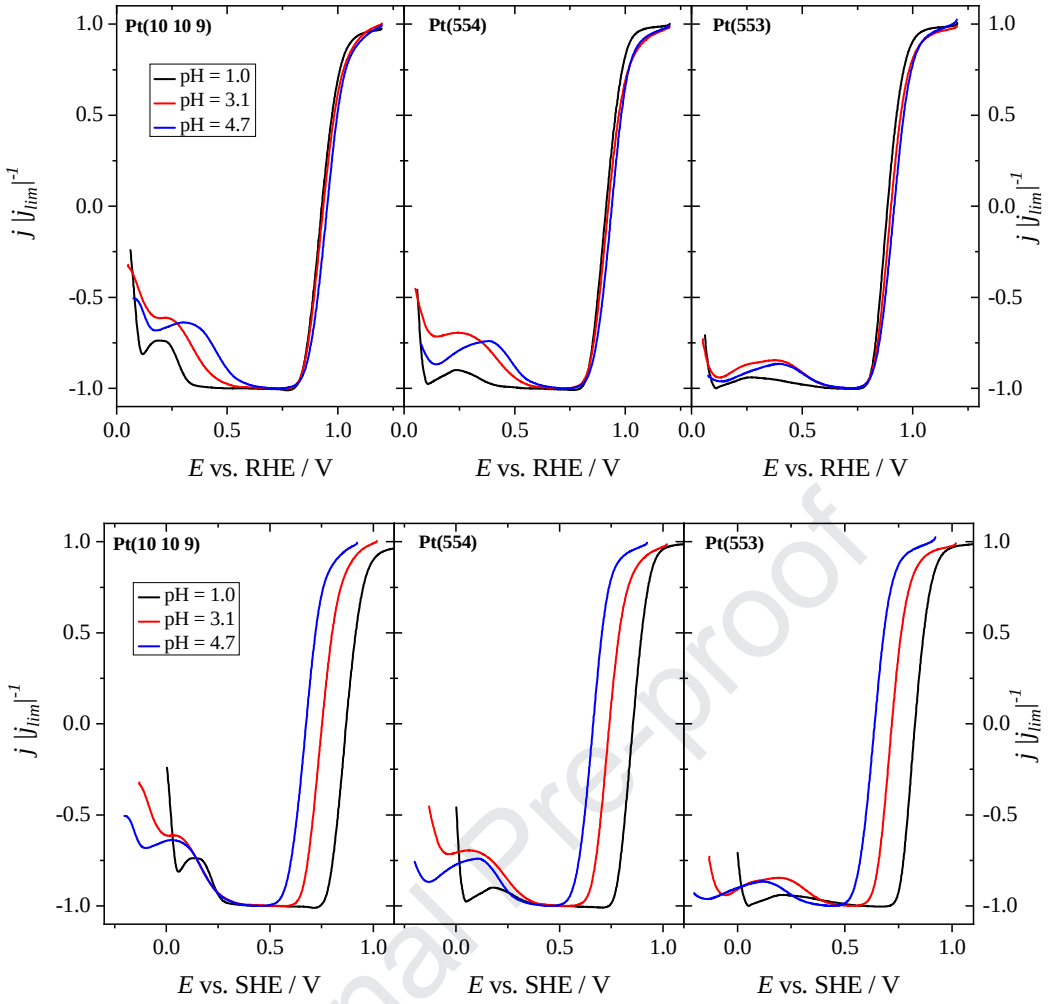

Figure 7: Normalized polarization curves for the HPRR and HPOR on different Pt(S)[(n-1)(111) × (110)] stepped surfaces in 1.7 mM H_2O_2 Ar-saturated solutions with different pH values prepared with NaF/$HClO_4$ mixtures in the RHE scale (top) and in the SHE scale (bottom); scan rate: 50 mV s^{-1}, rotation rate: 2500 rpm.

Regarding E_{peak}, the higher the solution pH is, the more positive E_{peak} is in the RHE scale. However, in this case, there is a non-Nernstian pH shift, on the contrary to $E_{inhibition}$ for terrace sites. Results in [30] pointed out that local pme values for step sites are located near the voltammetric step peak, and an apparent pH dependence for this peak different from the expected Nernstian shift (0.059 per pH unit in the SHE scale) is also observed on the studied surface orientations [19, 33-35]. Different explanations were proposed for this behavior: pH-dependent binding energy for hydrogen adsorption [34], a replacement of adsorbed hydrogen by adsorbed OH [33] or partial oxidation of water bounded to step sites [36]. A recent work in which different alkali cation solutions

are used in combination with DFT calculations supported the idea that a cation-hydroxyl co-adsorption exists leading to this non-Nernstian pH shift of the voltammetric peak traditionally ascribed to hydrogen adsorption [37]. In any case, it is clear from the present results that a direct correlation exists between the voltammetric step peak, the local step pme values and E_{peak} for hydrogen peroxide reduction.

Additional measurements were carried out at more alkaline pH values and are presented in figure 8. Results show that current densities reach the theoretical limiting value for Pt(776) at pH = 11.9 (figure 8A). Although this surface possesses very long terraces and therefore a high inhibition at low potential would be expected, almost no inhibition is observed. This should be related to the completely different surface charge properties at this pH, which in turn would cause important changes in the interfacial water structure. The current density values decrease to slightly lower values for Pt(111) in the case of pH = 12.9 (figure 8B). This could be due to difference in the structure of the interface, but since the pH is not markedly different, it could be also possible that in this pH hydrogen peroxide is predominantly in the basic OOH^- form which is negatively charged and thus its reactivity and its interaction with the surface can be different. It is worth mentioning that the different nature of the cations present in the solution could also have an influence in reactivity [38], especially in alkaline media, and future works will be carried out to study this possible effect.

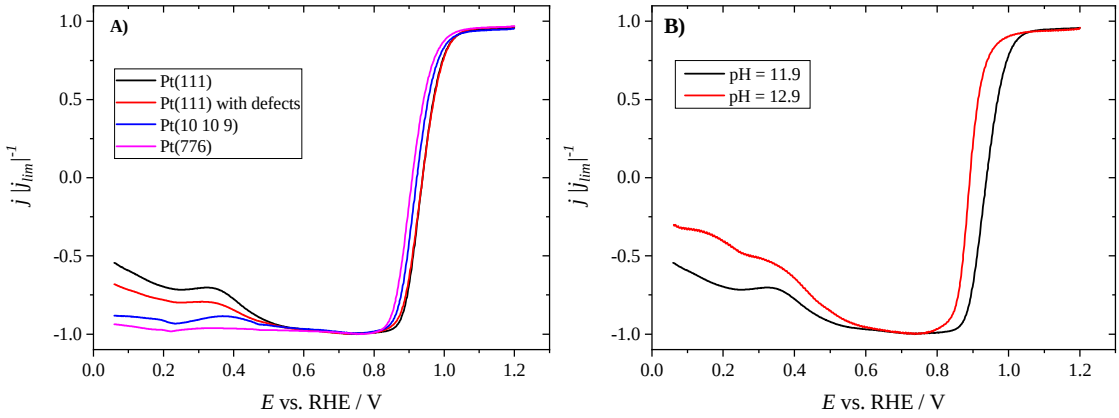

Figure 8: Normalized polarization curves for the HPRR and HPOR on different Pt(S)[(n-1)(111) × (110)] stepped surfaces in 1.7 mM H_2O_2 and 0.01 M NaOH + 0.09 M $KClO_4$ Ar-saturated solution (A) and on Pt(111) at two different alkaline pH values (B); scan rate: 50 mV s^{-1}, rotation rate: 2500 rpm. Original data prior to normalization are shown in Figure S5.

The dependence of $E_{inhibition}$ and E_{peak} with pH observed in this section further confirms their correspondence with the local pme for terraces and steps, respectively, of Pt stepped stepped surfaces. It can be also observed that adsorbed OH has a buffering effect which alters this correspondence when $E_{inhibition}$ is close to the potential of OH adsorption. This effect is especially dramatic in the case of Pt(110) and Pt(100), for which very similar polarization curves are obtained at the different studied pH values. In alkaline media, it is observed that at pH = 11.9 the inhibition is much lower, probably due to a more favorable effect of surface charge in this case.

Oxygen Reduction Reaction (ORR) and comparison with HPRR

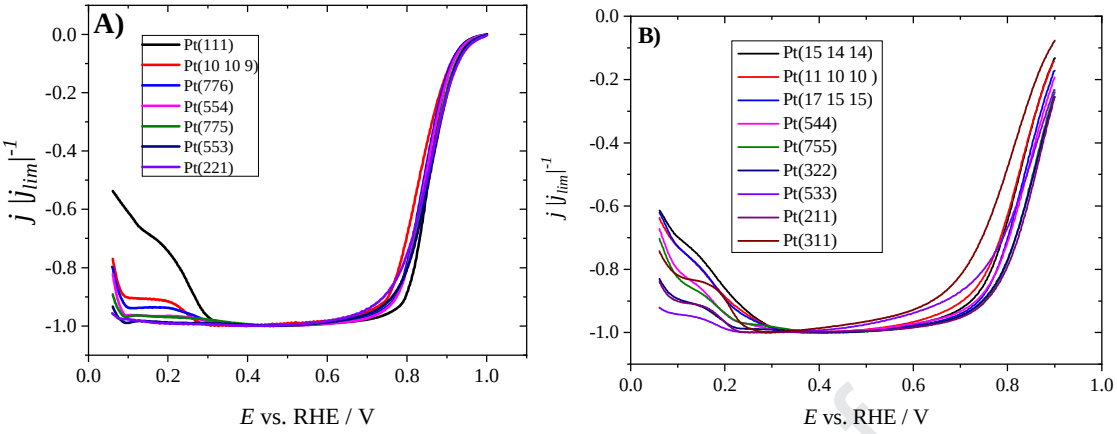

Figure 9: Normalized polarization curves for the ORR on different Pt(S)[(n-1)(111) × (110)] (A) and Pt[n(111) × (100)] (B) stepped surfaces in O_2-saturated 0.1 M $HClO_4$ solution; scan rate: 50 mV s^{-1}, rotation rate: 2500 rpm. Original data prior to normalization are shown in Figure S6.

The comparison between oxygen reduction reaction results and the previous data obtained from the HPRR can shed light on the ORR mechanism since hydrogen peroxide is a possible intermediate for this reaction. Figure 9 depicts the obtained results for ORR on Pt(S)[(n-1)(111) × (110)] and Pt(S)[n(111) × (100)] surfaces in 0.1 M $HClO_4$. Similar conclusions to the case of the HPRR can be deduced from these results: on the one hand, the addition of steps diminishes the inhibition at low potentials. On the other hand, $E_{inhibition}$ moves toward more positive values as step density is increased. However, some differences in comparison to HPRR can be highlighted. Firstly, the reduction peak at ca. 0.1 V vs. RHE for (110) steps and at ca. 0.27 V vs. RHE for (100) steps as a result of step activity is less defined than in the case of hydrogen peroxide reduction. In addition, the shift in $E_{inhibition}$ is only observable for (n-1) < 7 (where (n-1) is the number of atomic rows in the terrace when the step is considered to have (110) symmetry) in the case of Pt(S)[(n-1)(111) × (110)] surfaces and for Pt(S)[n(111) × (100)] surfaces $E_{inhibition}$ is even less discernible. That is, the inhibition for the ORR is lower than in the case of the HPRR since the inhibition is less

noticeable at potentials near the pzfc of terraces for the former one. These differences seem to indicate that although hydrogen peroxide is probably involved in the ORR as an intermediate species in these conditions, the mechanism does not take place via the total conversion of O_2 to H_2O_2 and subsequent reduction of the latter to water. In order to investigate the extent of H_2O_2 participation on the ORR mechanism, current density differences between ORR and HPRR on Pt(S)[(n-1)(111) × (110)] at different potential values in the region of reaction inhibition have been analyzed and presented in Figure 10. It is important to consider that for the ORR two electrons are transferred before the possible H_2O_2 intermediate formation and therefore a total inhibition means that current density is reduced to half the limiting current density. Hence, the difference between current density at a certain value and limiting current density was first calculated, and then the obtained value for ORR was doubled for the sake of comparison with that for the HPRR.

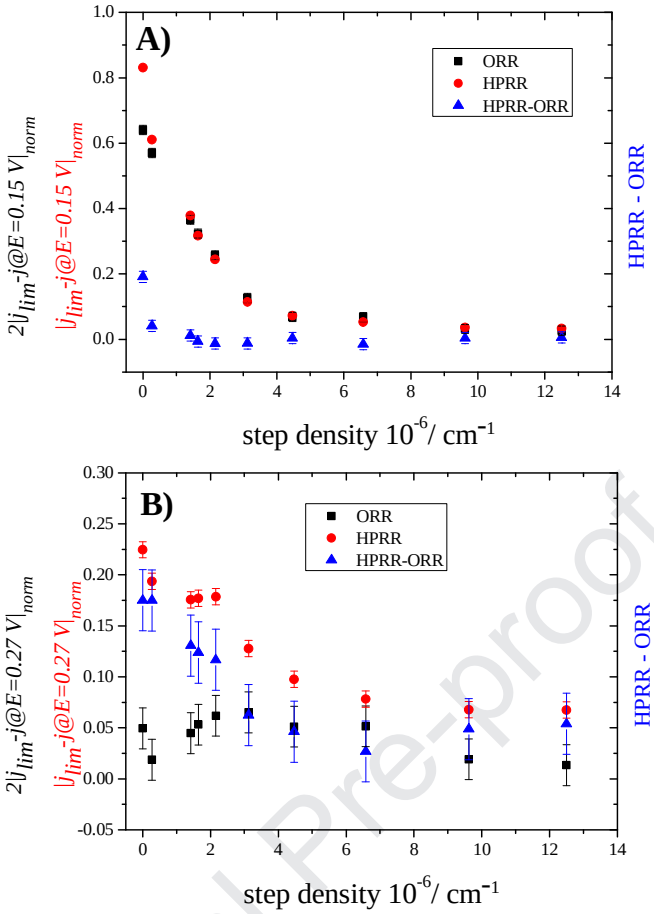

Figure 10: Difference between current density at 0.15 V vs. RHE (A) or 0.27 vs RHE (B) and limiting current density for HPRR (black) and ORR (red, in this case the value is multiplied by 2) and difference between values for both reactions (blue) for Pt(S)[(n-1)(111) × (110)] at 0.1 M $HClO_4$.

In the case of E = 0.15 V vs. RHE, differences between the inhibition in the ORR and HPRR are only discernible for Pt(111) or surfaces with very long terraces. At 0.15 V, the steps have an active role in the process, since the reduction in the current observed for the terraces is counterbalanced by the peak corresponding to the step sites. However, it is remarkable that, on Pt(111), the difference between both values is not negligible and the inhibition is higher for the HPRR than for the ORR. This would suggest that not all the initial O_2 molecules give rise to H_2O_2, but to other intermediate species which reactivity is different than hydrogen peroxide. For E = 0.27 V vs. RHE, differences are more pronounced and can be even observed for shorter terraces. The reason is that this potential value lies in the region where the inhibition on the (111)

terraces is starting, while the activity of steps remains constant. It can be observed that the inhibition is always higher for HPRR, and this difference increases as terraces are enlarged. This supports the fact that not all the O_2 molecules form the hydrogen peroxide intermediate and can give rise other intermediate or intermediates which are not inhibited near the pzfc of (111) terraces.

For achieving conditions in which differences between ORR and HPRR could be more noticeable, the ORR has been studied at solutions with less acidic pH values. When oxygen reduction reaction is studied on Pt(111) at different pH values, important differences in comparison with HPRR can be observed as can be seen in our previous work [19]. The most remarkable difference between the curves for both processes is that, at pH > 3, the limiting current density for the ORR decreases as pH is increased. Taking this fact into account, it was proposed that a bifurcation point exists previously to H_2O_2 formation since this behavior is not observed for the HPRR [19, 21]. Another point more directly related with the present study is that the inhibition at low potentials for the ORR does not move to more positive values when pH is increased, at least for the pH values where limiting current is not reduced. In fact, $E_{inhibition}$ moves toward more negative values until ca. 0.2 V for pH = 3. This completely different behavior between ORR and HPRR ($E_{inhibition}$ for the HPRR at pH = 3 is ca. 0.5 V vs. RHE) suggests that, as pH is increased, the formation of hydrogen peroxide is less favorable when compared with other possible intermediates, such as $OOH^{\bullet}$ as suggested in [19].

In order to get additional pieces of experimental evidence for this change in the mechanism between both reactions, the ORR was studied for Pt(S)[(n-1)(111) × (110)] surfaces at a pH value near 3 (Figure 11). This pH was selected because is the more positive value at which the decrease of limiting current density does not take place and therefore the inhibition at low potentials can be studied without the interference of this

effect. It can be observed that $E_{inhibition}$ for Pt(111) is considerably lower than the pzfc, and hence the ORR intermediate is not affected by the surface charge in the same way as H_2O_2 when the HPRR is studied. In addition, when step density is increased, only a small inhibition is observed at $E < 0.15$ V vs. RHE, and this behavior is drastically different to what is observed for the same surfaces when the HPRR is studied at these pH values. This is clearly illustrated in figure 12 for Pt(111) and Pt(775), showing the important differences for $E_{inhibition}$ between ORR and HPRR. All these results support the idea that there should be a bifurcation point in the mechanism before the formation of adsorbed H_2O_2, and the higher the pH is, the less favorable would be the pathway through the formation of H_2O_2.

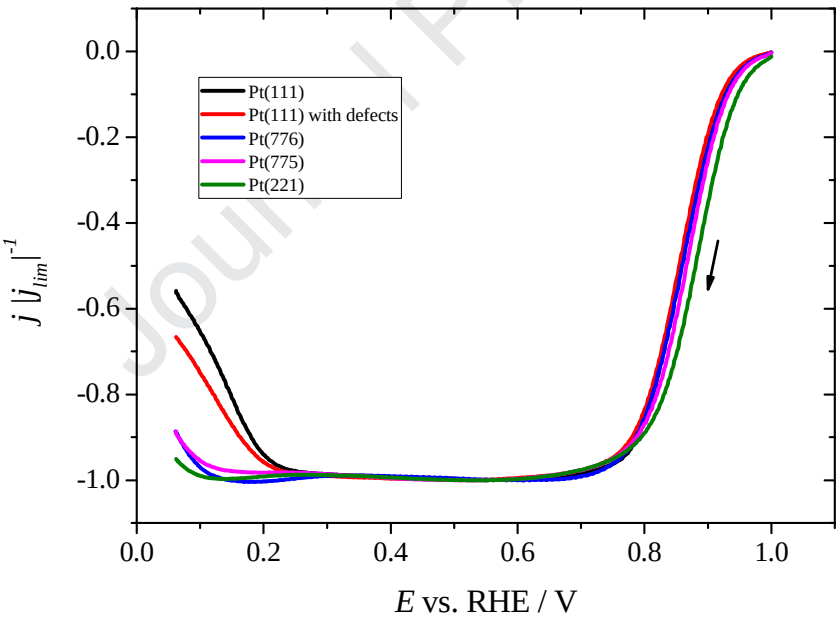

Figure 11: Normalized polarization curves for the ORR on different Pt[(n-1)(111) × (110)] stepped surfaces in O_2-saturated pH = 3 solution; scan rate: 50 mV s^{-1}, rotation rate: 2500 rpm. Original data prior to normalization are shown in Figure S7.

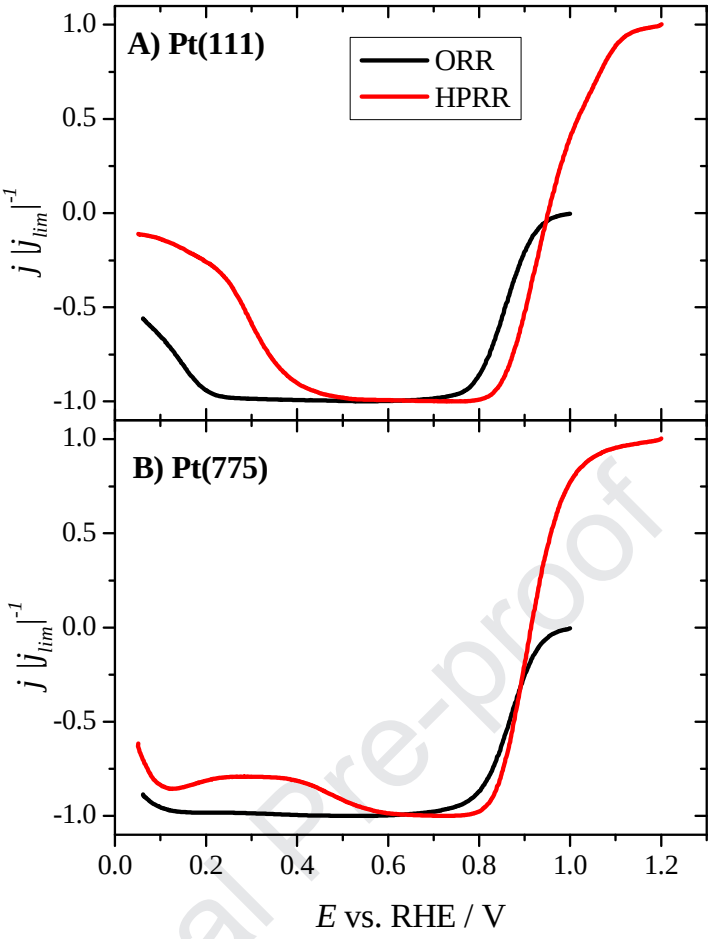

Figure 12: Polarization curves for the ORR and HPRR at pH = 3 on Pt(111) (A) and Pt(775) (b); scan rate: 50 mV s^{-1}, rotation rate: 2500 rpm.

The results obtained in this section evidence even more strongly the differences in the mechanism between the HPRR and the ORR. While $E_{inhibition}$ for the HPRR shifts to more positive values as the step density and/or the pH are increased, there is practically no inhibition at low potentials for the ORR on stepped surfaces at pH > 2.

4. Conclusions

Measurements for the HPRR for different Pt stepped surfaces in 0.1 M $HClO_4$ point out that there is a relationship between $E_{inhibition}$ of this reaction and the local pme, and therefore the pzfc, of the terraces of these surfaces. There is also a correlation between the reduction peak observed at low potential and the local pme for steps. These

results point out again the important influence of surface charge (and its influence on interfacial water) on the HPRR. Further measurements for the HPRR at other more neutral pH values confirm these relationships, since $E_{inhibition}$ for the HPRR for surfaces with long terraces shifts 0.059 V per pH unit to more positive potentials, as observed for the pme by laser-induced temperature-jump experiments [30]. However, for surfaces with high step density, since the local pme for terraces is at more positive potential values, the adsorption of OH starts to play a role at high pH values. The extreme cases are Pt(100) and Pt(110) because for these electrodes there is hydrogen and OH coadsorption at low potentials and OH adsorption has a strong influence on the water adlayer. Regarding E_{peak} of the peak due to H_2O_2 reduction at steps, the dependence with pH is not straight-forward, as well as the dependence of the pme, since there is a non-Nernstian shift of the voltammetric peak associated with steps. Further experiments in alkaline pH values reveal that from (n-1) = 13 there is already no inhibition at low potentials for pH = 11.9, suggesting a favorable effect of surface charge in this case.

From the comparison between the ORR and HPRR measurements, it can be deduced that not every O_2 molecule reacts to give H_2O_2, but a fraction of the O_2 molecules can react through another pathway because of the presence of a bifurcation point, probably involving $OOH^{\bullet}$ intermediate, before H_2O_2 formation. Studies at different pH with different surfaces suggest that the higher the pH of the solution is, the lower the formation of H_2O_2 intermediate is observed. This is in agreement with the previous conclusions extracted from the studies in the presence of bromide anion [20].

Acknowledgments

This work has been financially supported by the MICINN-FEDER (project CTQ2016-76221-P. VBM thankfully acknowledges to MINECO the award of a predoctoral grant (BES-2014-068176).

References

[1] A.M. Gómez-Marín, R. Rizo, J.M. Feliu, Oxygen reduction reaction at Pt single crystals: a critical overview, Catal. Sci. Technol., 4 (2014) 1685-1698.

[2] R.R. Adzic, Recent advances in the kinetics of oxygen reduction, in: J. Lipkowski, P.N. Ross (Eds.) Electrocatalysis, Wiley-VCH, New York, 1998, pp. 197-242.

[3] H.A. Gasteiger, N.M. Markovic, Just a dream or future reality?, Science, 324 (2009) 48-49.

[4] S. Guo, S. Zhang, S. Sun, Tuning nanoparticle catalysis for the oxygen reduction reaction, Angew. Chem. Int. Ed., 52 (2013) 8526-8544.

[5] J.K. Norskov, J. Rossmeisl, A. Logadottir, L. Lindqvist, J.R. Kitchin, T. Bligaard, H. Jonsson, Origin of the overpotential for oxygen reduction at a fuel-cell cathode, J. Phys. Chem. B, 108 (2004) 17886-17892.

[6] A.B. Anderson, T.V. Albu, Ab initio approach to calculating activation energies as functions of electrode potential. Trial application to four-electron reduction of oxygen, Electrochem. Commun., 1 (1999) 203-206.

[7] A.B. Anderson, T.V. Albu, Ab initio determination of reversible potentials and activation energies for outer-sphere oxygen reduction to water and the reverse oxidation reaction, J. Am. Chem. Soc., 121 (1999) 11855-11863.

[8] A. Panchenko, M.T.M. Koper, T.E. Shubina, S.J. Mitchell, E. Roduner, *Ab initio* calculations of intermediates of oxygen reduction on low-index platinum surfaces, J. Electrochem. Soc., 151 (2004) A2016-A2027.

[9] J.A. Keith, T. Jacob, Theoretical studies of potential-dependent and competing mechanisms of the electrocatalytic oxygen reduction reaction on Pt(111), Angew. Chem. Int. Edit., 49 (2010) 9521-9525.

[10] V. Tripković, E. Skúlason, S. Siahrostami, J.K. Nørskov, J. Rossmeisl, The oxygen reduction reaction mechanism on Pt(1 1 1) from density functional theory calculations, Electrochim. Acta, 55 (2010) 7975-7981.

[11] Y. Sha, T.H. Yu, B.V. Merinov, P. Shirvanian, W.A. Goddard, Oxygen hydration mechanism for the oxygen reduction reaction at Pt and Pd fuel cell catalysts, J. Phys. Chem. Lett., 2 (2011) 572-576.

[12] R. Jinnouchi, K. Kodama, T. Hatanaka, Y. Morimoto, First principles based mean field model for oxygen reduction reaction, Phys. Chem. Chem. Phys., 13 (2011) 21070-21083.

[13] V. Viswanathan, H.A. Hansen, J. Rossmeisl, J.K. Nørskov, Universality in oxygen reduction electrocatalysis on metal surfaces, ACS Catal., 2 (2012) 1654-1660.

[14] D. Fantauzzi, T. Zhu, J.E. Mueller, A.W.F. Filot, E.J.M. Hensen, T. Jacob, Microkinetic modeling of the oxygen reduction reaction at the Pt(111)/gas interface, Catal. Lett., 145 (2015) 451-457.

[15] N.M. Markovic, P.N. Ross, Surface science studies of model fuel cell electrocatalysts, Surf. Sci. Rep., 45 (2002) 117-229.

[16] E. Yeager, Electrocatalysts for O_2 reduction, Electrochim. Acta, 29 (1984) 1527-1537.

[17] A.M. Gómez-Marín, J.M. Feliu, New insights into the oxygen reduction reaction mechanism on Pt(111): a detailed electrochemical study, ChemSusChem, 6 (2013) 1091-1100.

[18] A.M. Gomez-Marín, J.M. Feliu, E.A. Ticianelli, On the reaction mechanism for oxygen reduction on platinum: Existence of a fast initial chemical step and soluble species different to H_2O_2, ACS Catal., 8 (2018) 7931-7943.

[19] V. Briega-Martos, E. Herrero, J.M. Feliu, Effect of pH and water structure on the oxygen reduction reaction on platinum electrodes, Electrochim. Acta, 241 (2017) 497-509.

[20] V. Briega-Martos, G.A.B. Mello, R.M. Arán-Ais, V. Climent, E. Herrero, J.M. Feliu, Understandings on the inhibition of oxygen reduction reaction by bromide adsorption on Pt(111) electrodes at different pH values, J. Electrochem. Soc., 165 (2018) J3045-J3051.

[21] V. Briega-Martos, E. Herrero, J.M. Feliu, The inhibition of hydrogen peroxide reduction at low potentials on Pt(111): Hydrogen adsorption or interfacial charge?, Electrochem. Commun., 85 (2017) 32-35.

[22] P. Sebastián, R. Martínez-Hincapié, V. Climent, J.M. Feliu, Study of the Pt(111) | electrolyte interface in the region close to neutral pH solutions by the laser induced temperature jump technique, Electrochim. Acta, 228 (2017) 667-676.

[23] J.-C. Dong, X.-G. Zhang, V. Briega-Martos, X. Jin, J. Yang, S. Chen, Z.-L. Yang, D.-Y. Wu, J.M. Feliu, C.T. Williams, Z.-Q. Tian, J.-F. Li, In situ Raman spectroscopic evidence for oxygen reduction reaction intermediates at platinum single-crystal surfaces, Nat. Energy, 4 (2019) 60-67.

[24] S. Nayak, I.J. McPherson, K.A. Vincent, Adsorbed intermediates in oxygen reduction on platinum nanoparticles observed by in situ IR spectroscopy, Angew. Chem. Int. Edit., 57 (2018) 12855-12858.

[25] C. Korzeniewski, V. Climent, J.M. Feliu, Electrochemistry at Platinum Single Crystal Electrodes, in: A.J. Bard, C. Zoski (Eds.) Electroanalytical Chemistry: A Series of Advances, CRC Press, Boca Raton, 2012, pp. 75-169.

[26] J. Clavilier, D. Armand, S.G. Sun, M. Petit, Electrochemical adsorption behaviour of platinum stepped surfaces in sulphuric acid solutions J. Electroanal. Chem., 205 (1986) 267-277.

[27] J.M. Feliu, A. Rodes, J.M. Orts, J. Clavilier, The problem of surface order of Pt single-crystals in electrochemistry, Polish Journal of Chemistry, 68 (1994) 1575-1595.

[28] E. Sitta, A.M. Gomez-Marin, A. Aldaz, J.M. Feliu, Electrocatalysis of H_2O_2 reduction/oxidation at model platinum surfaces, Electrochem. Commun., 33 (2013) 39-42.

[29] V. Climent, N. Garcia-Araez, E. Herrero, J. Feliu, Potential of zero total charge of platinum single crystals: A local approach to stepped surfaces vicinal to Pt(111), Russ. J. Electrochem., 42 (2006) 1145-1160.

[30] N. Garcia-Araez, V. Climent, J.M. Feliu, Potential-dependent water orientation on Pt(111) stepped surfaces from laser-pulsed experiments, Electrochim. Acta, 54 (2009) 966-977.

[31] V. Climent, G.A. Attard, J.M. Feliu, Potential of zero charge of platinum stepped surfaces: a combined approach of CO charge displacement and N_2O reduction, J. Electroanal. Chem., 532 (2002) 67-74.

[32] R. Martínez-Hincapié, V. Climent, J.M. Feliu, Peroxodisulfate reduction as a probe to interfacial charge, Electrochem. Commun., 88 (2018) 43-46.

[33] M.J.T.C. van der Niet, N. Garcia-Araez, J. Hernández, J.M. Feliu, M.T.M. Koper, Water dissociation on well-defined platinum surfaces: The electrochemical perspective, Catal. Today, 202 (2013) 105-113.

[34] W. Sheng, Z. Zhuang, M. Gao, J. Zheng, J.G. Chen, Y. Yan, Correlating hydrogen oxidation and evolution activity on platinum at different pH with measured hydrogen binding energy, Nature Commun., 6 (2015) 5848-5853.

[35] M.J.S. Farias, G.A.B. Mello, A.A. Tanaka, J.M. Feliu, Site-specific catalytic activity of model platinum surfaces in different electrolytic environments as monitored by the CO oxidation reaction, J. Catal., 345 (2017) 216-227.

[36] K. Schwarz, B. Xu, Y. Yan, R. Sundararaman, Partial oxidation of step-bound water leads to anomalous pH effects on metal electrode step-edges, Phys. Chem. Chem. Phys., 18 (2016) 16216-16223.

[37] X. Chen, I.T. McCrum, K. Schwarz, M.J. Janik, M.T.M. Koper, Co-adsorption of cations as the cause of the apparent pH dependence of hydrogen adsorption on a stepped platinum single-crystal electrode, Angew. Chem. Int. Ed., 56 (2017) 15025-15029.

[38] D. Strmcnik, K. Kodama, D. van der Vliet, J. Greeley, V.R. Stamenkovic, N.M. Marković, The role of non-covalent interactions in electrocatalytic fuel-cell reactions on platinum, Nat. Chem., 1 (2009) 466-472.

V. Briega-Martos has carried out the experimental work

E. Herrero and J.M. Feliu have devised and guided the experimental work

All authors have contributed in the analysis and writing of the manuscript.

Declaration of interests

☒ The authors declare that they have no known competing financial interests or personal relationships that could have appeared to influence the work reported in this paper.

☐The authors declare the following financial interests/personal relationships which may be considered as potential competing interests: